IOP Publishing Journal of Physics: Condensed Matter
J. Phys.: Condens. Matter **34** (2022) 275603 (7pp) https://doi.org/10.1088/1361-648X/ac699f

Half-topological state in magnetic topological insulators

Minh-Tien Tran* **and Thanh-Mai Thi Tran**

Institute of Physics, Vietnam Academy of Science and Technology, Hanoi 10072, Vietnam

E-mail: minhtien@iop.vast.vn

Received 6 January 2022, revised 12 April 2022
Accepted for publication 22 April 2022
Published 11 May 2022

Abstract

We predict a novel topological state, *half-topological state*, in magnetic topological insulators. The topological state is characterized by different topologies of electrons with different spin orientations, i.e., electrons with one spin orientation occupy a nontrivial topological insulating state, while electrons with opposite orientation occupy another insulating state with trivial topology. We demonstrate the occurrence of the half-topological state in magnetic topological insulators by employing a minimal model. The minimal model is a combination of the spinful Haldane and the double-exchange models. The double-exchange processes maintain a spontaneous magnetic ordering, while the next-nearest-neighbor hopping in the Haldane model gives rise to a nontrivial topological insulator. The minimal model is studied by applying the dynamical mean field theory. It is found that the long-range antiferromagnetic ordering drives the system from either topological or topologically trivial antiferromagnetic insulator to the half-topological state, and finally to topologically trivial antiferromagnetic insulator. The equations for the topological phase transitions are also explicitly derived.

Keywords: magnetic topological insulator, topological phase transition, topologically breaking of spin symmetry, electron correlations

(Some figures may appear in colour only in the online journal)

1. Introduction

Since the discovery of magnetic topological insulators (MTIs), the interplay between a long-range magnetic ordering and topology has attracted a lot of research attention [1–5]. While the magnetic ordering is established by a symmetry breaking within the Landau phase theory, topology of the ground state is beyond the theory of symmetry breaking. The magnetic ordering may intriguingly impact on the topology of the ground state, and as a result exotic states may emerge [6, 7]. In MTIs the anomalous Hall conductivity is quantized, and it coexists with magnetism of the materials. The quantization of the Hall conductance manifests a nontrivial topology of the ground state [8, 9]. In paramagnetic (PM) topological insulators (TIs), electrons with both spin orientations simultaneously form the topological ground state. For example, in two-dimensional $\mathcal{Z}_2$ TIs, electrons of both spin orientations occupy the lowest spin-degenerate energy bands, and these occupied bands for each spin orientation give equal quantized amounts to the Hall conductivity but with opposite signs [10]. As a consequence, the spin Hall conductivity is quantized, while the charge Hall conductivity vanishes. Within the Kane–Mele model of the $\mathcal{Z}_2$ TI, electrons of both spin orientations simultaneously are in either nontrivial or trivial topological insulating state [10]. In ferromagnetic (FM) materials, the spin-degenerate bands are split by the FM magnetization. Electrons are magnetically polarized, and electrons of one spin orientation dominantly occupy the lowest energy bands, while electrons of opposite spin orientation dominantly occupy the higher-energy split bands. Since the FM magnetization can play like an external magnetic field, the anomalous Hall effect can occur in FM materials [1, 2]. In ferromagnetic topological insulators (FMTIs), the lowest energy bands are occupied by electrons with the polarized spin, and the ground state is topologically nontrivial [1, 2]. Although electrons with opposite spin orientation may not occupy the topological ground state, the higher-energy split band that is occupied by them

* Author to whom any correspondence should be addressed.

is still topologically nontrivial. Therefore, both spin orientations of electrons in FMTIs are magnetically inequivalent, but they are simultaneously in the nontrivial topological state. In FMTIs both spin orientations are topologically symmetry. The topological symmetry of the spin orientations also occurs in antiferromagnetic topological insulators (AFTIs) [11, 12]. In AFTIs electrons of both spin components occupy the topological ground state, although their sublattice magnetizations have opposite values. The occupied bands for each spin component contribute a quantized value to the Hall conductivity, therefore electrons of both spin orientations are simultaneously topological [11, 12].

In this paper, we show a possibility of topologically breaking of the spin symmetry in MTIs, i.e. electrons with opposite spin orientations occupy the insulating states with different topologies, for instance, electrons with one spin orientation occupy a nontrivial topological insulating state, while electrons with opposite spin orientation occupy another insulating state with trivial topology. This state is reminiscent to the half-metallic state, where electrons of one spin orientation are metallic, while electrons of opposite spin orientation are insulating [14, 15]. In mimicking the half-metallic state, we refer to the state with topologically breaking of the spin symmetry as half-topological state. The half-topological state was previously found in correlated TIs by employing topological insulator models with the Hubbard interaction [16–19]. It appears as an emergence of the long-range antiferromagnetic (AFM) ordering and the lack of the lattice inversion symmetry [16–19]. However, in the previous studies, the magnetic topological state is absent and electron correlations drive the system only from either the PM (topological or normal) or topologically trivial AFM state to the half-topological state [16–19]. In contrast, in this paper we will specially show the existence of the half-topological state in MTIs. The long-range AFM ordering can drive the system from the topological or topologically trivial AFM insulator to the half-topological state, and then to the topologically trivial AFM insulator. Such topological phase transitions are absent in the previous studies [16–19]. We will demonstrate the topological phase transition in MTIs by employing a minimal model. The minimal model is a combination of the spinful Haldane and the double-exchange models. The spinful Haldane model is a spin generalization of the Haldane one [13]. It was introduced to study the interplay between correlation and topology in systems without the time-reversal symmetry [20–24]. The spinful Haldane model consists of two identical Haldane models, each of which describes the dynamics of electrons of one spin orientation. The ionic potential, which breaks the lattice inversion symmetry, can drives the system from topological to normal insulator [13]. The double exchange model describes the Hund coupling between itinerant electrons and magnetic moments [25–27]. The Hund coupling generates the double exchange processes between electrons and magnetic moments, that cause a spontaneous magnetic ordering. Including the Hund coupling into the spinful Haldane model, it can describe both magnetism and topology in systems without the time-reversal symmetry. This contrasts to the including the Hund coupling to the Kane–Mele model, which preserves the time-reversal symmetry [11, 12]. The interplay between magnetism and topology in the proposed model is studied by applying the dynamical mean field theory (DMFT) [28, 29]. The DMFT has widely and successfully been used to study correlated electron systems, and in particular the double exchange model [30–39]. By using the topological Green function [40, 41], we derive the equations that determine the phase transition of the half-topological state. They show that the AFM ordering and the breaking of the lattice inversion symmetry are necessary, but not sufficient for the existence of the half-topological state. In contrast to the previous studies, where the half-topological state transition can occur at the phase boundary of the magnetic phase transition [16–19], the stability of the half-topological state in MTIs requires a finite AFM magnetization, therefore the topological phase transition occurs after the magnetic phase transition takes place.

The rest of the paper is organized as follows. In section 2 we describe the model and its DMFT. The numerical results are presented in section 3. Finally, section 4 is the conclusion.

2. Model

We study the interplay between magnetism and topology in MTIs by employing a minimal model. The minimal model is a combination of the spinful Haldane and the double-exchange models. It consists of itinerant electrons, hopping on a honeycomb lattice, and localized magnetic impurities. Its Hamiltonian can be written as

$$H = -t\sum_{\langle i,j\rangle,\sigma} c^{\dagger}_{i\sigma}c_{j\sigma} - t_2\sum_{\langle\langle i,j\rangle\rangle,\sigma} \mathrm{e}^{\mathrm{i}\phi_{ij}}c^{\dagger}_{i\sigma}c_{j\sigma} - \frac{\Delta}{2}\sum_{i\sigma}\epsilon_i c^{\dagger}_{i\sigma}c_{i\sigma} - J\sum_{i,ss'}\mathbf{S}_i c^{\dagger}_{is}\boldsymbol{\sigma}_{ss'}c_{is'}, \quad (1)$$

where $c^{\dagger}_{i\sigma}$ ($c_{i\sigma}$) is the creation (annihilation) operator of electron. The subscripts i and σ denote the lattice site and spin of electrons. The honeycomb lattice is divided into two penetrating sublattices a and b, and $\langle i,j\rangle$ ($\langle\langle i,j\rangle\rangle$) denotes the nearest-neighbor (next-nearest-neighbor) lattice sites. t (t_2) is the nearest-neighbor (next-nearest-neighbor) hopping parameter. ϕ_{ij} is the Peierls phase that is acquired by electron hopping in a zero total magnetic flux, but with finite sublattice fluxes [13]. Without loss of generality, we consider the case $\phi_{ij} = \pm\pi/2$ for anticlockwise (clockwise) hopping. Δ is a staggered ionic potential and $\epsilon_i = \pm 1$ when lattice site i belongs to the sublattice a (b). The ionic potential breaks the lattice inversion symmetry. $\mathbf{S}_i$ is spin of magnetic impurity at lattice site i. $\boldsymbol{\sigma} = (\sigma^x, \sigma^y, \sigma^z)$ are the Pauli matrices. J is the Hund couping between itinerant electrons and magnetic impurities. For simplicity, we will consider the FM case $J > 0$, and treat $\mathbf{S}_i$ as a classical spin with the norm $\mathbf{S}_i^2 = 1$. When the Hund coupling is FM ($J > 0$), there is no significant difference between the quantum and classical spin cases [42]. The first two terms in Hamiltonian (1) are the spinful Haldane model, where each spin component term describes the fermion hopping on the honeycomb lattice with zero total flux [13]. The next-nearest-neighbor hopping opens a gap and induces a topological state

when $\Delta < 6\sqrt{3}t_2$ [13]. When $t_2 = 0$ and $\Delta = 0$, Hamiltonian (1) describes the double exchange model [25–27]. The Hund coupling drives the system from PM to magnetic state. In the absence of the ionic potential ($\Delta = 0$), both nontrivial topology and magnetism may simultaneously occur [11, 12]. However, as we will show, when the inversion symmetry is present ($\Delta = 0$), electrons with both spin orientations simultaneously form either topological or normal insulator. When the ionic potential is present ($\Delta \neq 0$), its interplay with magnetism may topologically break the spin symmetry and results in a half-topological state.

The magnetic ground state can be analyzed in the strong coupling regime $J \gg t, t_2$. The classical spin of magnetic impurities can be presented as

$$\mathbf{S}_i = (\cos\,\varphi_i\,\sin\,\theta_i, \sin\,\varphi_i\,\sin\,\theta_i, \cos\,\theta_i), \tag{2}$$

where θ_i and φ_i are the polar and azimuthal angles of spin $\mathbf{S}_i$. Performing the unitary transform [27]

$$\hat{f}_i \equiv \begin{pmatrix} f_{i\uparrow} \\ f_{i\downarrow} \end{pmatrix} = \mathbf{U} \begin{pmatrix} c_{i\uparrow} \\ c_{i\downarrow} \end{pmatrix}, \tag{3}$$

with the unitary matrix

$$\mathbf{U} = \begin{pmatrix} \cos(\theta_i/2) & \sin(\theta_i/2)\mathrm{e}^{-\mathrm{i}\varphi_i} \\ -\sin(\theta_i/2)\mathrm{e}^{\mathrm{i}\varphi_i} & \cos(\theta_i/2) \end{pmatrix}, \tag{4}$$

we obtain

$$H_{\mathrm{Hund}} = -2J \sum_{i,ss'} \mathbf{S}_i \cdot \mathbf{s}_i = -J \sum_{i,\sigma} \sigma f^\dagger_{i\sigma} f_{i\sigma}, \tag{5}$$

where $\mathbf{s}_i = (1/2)\sum_{ss'} c^\dagger_{is}\boldsymbol{\sigma}_{ss'}c_{is'}$ is the spin of itinerant electrons. In the new basis the Hund coupling is diagonal. It prefers the magnetization in the z-axis direction. After the unitary transform, the hopping terms in Hamiltonian (1) become

$$H_{\mathrm{hop}} = -t \sum_{\langle i,j\rangle} \hat{f}^\dagger_i \hat{T}_{ij} \hat{f}_j + t_2 \sum_{\langle\langle i,j\rangle\rangle} \mathrm{e}^{\mathrm{i}\phi_{ij}} \hat{f}^\dagger_i \hat{T}_{ij} \hat{f}_j, \tag{6}$$

where

$$\hat{T}_{ij} = \begin{pmatrix} \cos\dfrac{\theta_i}{2}\cos\dfrac{\theta_j}{2} + \sin\dfrac{\theta_i}{2}\sin\dfrac{\theta_j}{2}\mathrm{e}^{-\mathrm{i}(\varphi_i-\varphi_j)} & -\cos\dfrac{\theta_i}{2}\sin\dfrac{\theta_j}{2}\mathrm{e}^{-\mathrm{i}\varphi_j} + \sin\dfrac{\theta_i}{2}\cos\dfrac{\theta_j}{2}\mathrm{e}^{-\mathrm{i}\varphi_i} \\ -\sin\dfrac{\theta_i}{2}\cos\dfrac{\theta_j}{2}\mathrm{e}^{\mathrm{i}\varphi_i} + \cos\dfrac{\theta_i}{2}\sin\dfrac{\theta_j}{2}\mathrm{e}^{\mathrm{i}\varphi_j} & \cos\dfrac{\theta_i}{2}\cos\dfrac{\theta_j}{2} + \sin\dfrac{\theta_i}{2}\sin\dfrac{\theta_j}{2}\mathrm{e}^{\mathrm{i}(\varphi_i-\varphi_j)} \end{pmatrix}.$$

In contrast to the Kane–Mele model [11], in the spinfull Haldane model both the nearest-neighbor and next-nearest-neighbor hoppings have the same hopping matrix $\hat{T}_{ij}$. For simplicity, we consider the ground state, where the impurity spins have the same azimuthal angle $\varphi_i = \varphi$. In the strong coupling regime, electrons with one spin orientation are relevant to the ground state, and their nearest-neighbor hopping is maximal when $\theta_a - \theta_b = 0$ or π. This is equivalent to the parallel or antiparallel aligning of the nearest-neighbor spins. When the spin orientations at the nearest-neighbor sites are parallel or antiparallel, the off-diagonal elements of the hopping matrix $\hat{T}_{ij}$ vanish. This is actually the double exchange mechanism, where spins align parallel or antiparallel in order to minimize the kinetic energy. Because in the ground state the off-diagonal elements of the hopping matrix $\hat{T}_{ij}$ vanish, the spins of itinerant electrons are ordered in the z-axis direction. On the other hand, Hamiltonian (1) conserves the total spin $\mathbf{S}_t = \sum_i(\mathbf{S}_i + \mathbf{s}_i)$ and its z-component S^z_t. The double-exchange mechanism favours the state with maximal S^z_t or $S^z_t = 0$. This also implies that the spins of magnetic impurities and itinerant electrons also align parallel.

The dynamics of interacting systems can be analyzed by using the Green function. Since the proposed model (1) has both spin and sublattice degrees of freedom, the single-particle Green function can be defined by

$$\hat{G}(\mathbf{k}, \tau) = -\langle \mathcal{T}\Psi_{\mathbf{k}}(\tau)\Psi^\dagger_{\mathbf{k}}\rangle, \tag{7}$$

where $\Psi^\dagger_{\mathbf{k}} = (c^\dagger_{\mathbf{k}a\uparrow}, c^\dagger_{\mathbf{k}b\uparrow}, c^\dagger_{\mathbf{k}a\downarrow}, c^\dagger_{\mathbf{k}b\downarrow})$. It satisfies the Dyson equation

$$\hat{G}(\mathbf{k}, z) = \left[z - \hat{H}_0(\mathbf{k}) - \hat{\Sigma}(\mathbf{k}, z)\right]^{-1}, \tag{8}$$

where $\hat{H}_0(\mathbf{k})$ is the non-interacting Bloch Hamiltonian, and $\hat{\Sigma}(\mathbf{k}, z)$ is the self energy, which contains all interacting effects. The non-interacting Bloch Hamiltonian is diagonal in the spinor space

$$\hat{H}_0(\mathbf{k}) = \hat{h}(\mathbf{k}) \times \hat{1}, \tag{9}$$

where $\hat{h}(\mathbf{k})$ is the non-interacting Bloch Hamiltonian for one spin component

$$\hat{h}(\mathbf{k}) = \begin{pmatrix} -t_2\xi_{\mathbf{k}} - \Delta/2 & -t\gamma_{\mathbf{k}} \\ -t\gamma^*_{\mathbf{k}} & t_2\xi_{\mathbf{k}} + \Delta/2 \end{pmatrix},$$

and $\hat{1}$ is the unique matrix in the spinor space. Here we use the following notations: $\gamma_{\mathbf{k}} = \sum_\delta \mathrm{e}^{\mathrm{i}\mathbf{k}\cdot\mathbf{r}_\delta}$, $\xi_{\mathbf{k}} = \sum_\eta \mathrm{e}^{\mathrm{i}\phi_\eta}\,\mathrm{e}^{\mathrm{i}\mathbf{k}\cdot\mathbf{r}_\eta}$, where δ and η denotes nearest-neighbor and next-nearest-neighbor sites of a given site, respectively. $\hat{h}(\mathbf{k})$ is exactly the Bloch Hamiltonian of the Haldane model [13]. In the non-interacting case, electrons of both spin components have the identical dynamics. The ground state changes from topological to normal insulating state at $\Delta_c = 6\sqrt{3}t_2$ [13].

We use the DMFT to calculate the Green function and its self energy [28, 29]. The DMFT exactly treats the local dynamics of electrons, but it neglects non-local spacial correlations. Within the DMFT, the self

energy depends only on frequency. In addition, the self energy is also diagonal in the spin and sublattice indices, i.e., $\hat{\Sigma}(\mathbf{k},z)=\mathrm{diag}[\Sigma_{a\uparrow}(z),\Sigma_{b\uparrow}(z),\Sigma_{a\downarrow}(z),\Sigma_{b\downarrow}(z)]$, because the double-exchange mechanism favours the magnetic ordering in the z-axis direction. The self energy $\Sigma_{\alpha\sigma}(z)$ is calculated from an effective single site of the α-sublattice embedded in a self-consistent dynamical mean field [29]. The action of the effective single-site dynamics reads

$$\begin{aligned}\mathcal{S}_\alpha=&-\sum_s\int_0^\beta\int_0^\beta \mathrm{d}\tau\,\mathrm{d}\tau'\Psi^\dagger_{\alpha s}(\tau)\mathcal{G}^{-1}_{\alpha s}(\tau-\tau')\Psi_{\alpha s}(\tau')\\&-\frac{\Delta_\alpha}{2}\sum_s\int_0^\beta \mathrm{d}\tau\epsilon_\alpha\Psi^\dagger_{\alpha s}(\tau)\Psi_{\alpha s}(\tau)\\&-J\sum_{\alpha ss'}\int_0^\beta \mathrm{d}\tau\mathbf{S}_\alpha(\tau)\Psi^\dagger_{\alpha s}(\tau)\boldsymbol{\sigma}_{ss'}\Psi_{\alpha s'}(\tau),\end{aligned}\tag{10}$$

where $\mathcal{G}^{-1}_{\alpha s}(z)=[\sum_{\mathbf{k}}\hat{G}(\mathbf{k},z)]^{-1}_{\alpha s,\alpha s}-\Sigma_{\alpha s}(z)$ is the cavity Green function which represents the dynamical mean field at a site of the sublattice α ($\alpha=a,b$). For classical spin $\mathbf{S}_\alpha$, the action (10) can exactly be solved, and once it is solved, we obtain the local Green function and its self energy [11]. The self-consistent condition of the DMFT requires that the local self energy obtained from the action (10) coincides with the αs-th component of the lattice self energy $\hat{\Sigma}(z)$. Once the self energy and the Green function are obtained, we can compute the sublattice magnetization and determine the magnetic type of the ground state. The sublattice magnetization is determined by

$$m_\alpha=\frac{1}{2N}\sum_{\mathbf{k},\sigma}\sigma\langle c^\dagger_{\mathbf{k}\alpha\sigma}c_{\mathbf{k}\alpha\sigma}\rangle,\tag{11}$$

which can directly be calculated from the Green function (8). The ground state is AFM when $m_a=-m_b\neq 0$. The topology of the ground state is determined by the Chern number. Within the DMFT, the self energy are diagonal in the spin space, therefore the Chern number can be defined with each spin component of electrons. The Chern number of αth band in the spin sector σ is determined by

$$C_{\sigma\alpha}=\frac{1}{2\pi}\int \mathrm{d}^2k\mathcal{F}_{\sigma\alpha}(\mathbf{k}),\tag{12}$$

where $\mathcal{F}_{\sigma\alpha}(\mathbf{k})=\partial_x\mathcal{A}_{\sigma\alpha y}-\partial_y\mathcal{A}_{\sigma\alpha x}$, $\mathcal{A}_{\sigma\alpha x(y)}=i\langle\Phi_{\sigma\alpha}(\mathbf{k})|\partial_{k_{x(y)}}|\Phi_{\sigma\alpha}(\mathbf{k})\rangle$, and $|\Phi_{\sigma\alpha}(\mathbf{k})\rangle$ is the orthonormalized eigenstate of the topological Bloch Hamiltonian $\hat{H}_t(\mathbf{k})=\hat{H}_0(\mathbf{k})+\hat{\Sigma}(i0)$ in the spin sector σ [43–45]. Equation (12) is a generalization of the Thouless–Kohmoto–Nightingale–Nijs (TKNN) formula for interacting systems. It can efficiently be calculated in discretized Brillouin zone [46]. In determining the ground-state topology the topological Bloch Hamiltonian $\hat{H}_t(\mathbf{k})$ plays the same role as the Bloch Hamiltonian $\hat{H}_0(\mathbf{k})$ in the non-interacting case.

3. Numerical results

We will study the magnetic and topological properties of the system at half filling. The ground state at half filling is insulating. First, we consider the case $\Delta=0$. In this case the model has the lattice inversion symmetry. The sublattice magnetizations and the Chern number for each spin orientation are presented in figure 1(a) as functions of the Hund coupling J. The Hund coupling drives the system from PM to AFM state. J_m is the critical value of that phase transition. The double exchange processes generated by the Hund coupling induce the magnetic ordering in order to minimize the kinetic energy [25–27]. The next-nearest-neighbor hopping t_2 does not qualitatively change the magnetic phase transition. Figure 1(a) also shows that the Chern number $C_\sigma=1$ when $J<J_c$. The Hund coupling also drives the system from nontrivial ($C_\sigma=1$) to trivial ($C_\sigma=0$) topological state. In this topological phase transition electrons of both spin orientations are simultaneously in either topological or normal insulating state. However, the topological phase transition occurs after the AFM phase transition takes place. Therefore in the range $J_m<J<J_c$, the ground state is AFM and topologically nontrivial. It yields an AFM topological state. This contrasts the Haldane–Hubbard model, where there is no intermediate AFM topological state between the topological PM and the topologically trivial AFM states [16].

When the sublattice potential is included ($\Delta\neq 0$), the lattice inversion symmetry is broken. In the non-interacting case ($J=0$), the ionic potential Δ drives the system from topological to normal insulator [13]. The topological phase transition occurs at $\Delta_c=6\sqrt{3}t_2$. In figure 1 we also plot the dependence of the sublattice magnetizations and the Chern numbers on the Hund coupling in both cases $\Delta<\Delta_c$ and $\Delta>\Delta_c$. The non-interacting ground state is a topological insulator with the Chern number $C_\sigma=1$ when $\Delta<\Delta_c$, and is a normal insulator with the Chern number $C_\sigma=0$ when $\Delta>\Delta_c$. When the Hund coupling is finite, the ionic potential does not qualitatively change the sublattice magnetizations, but it significantly impacts on the Chern numbers. It splits the topological phase transition point J_c into J_{c1} and J_{c2} for each spin orientation, as shown in figures 1(b) and (c). As a consequence, in the range $J_{c1}<J<J_{c2}$, electrons with different spin orientations have different topologies. Electrons with spin up are in trivial topological state, while electrons with spin down are in nontrivial one. This is a half-topological state. We find that $J_{c2}>J_{c1}>J_m$. This implies that the half-topological state only occurs in the AFM state. The AFM magnetization drives the system from either topological or topologically trivial AFM state to the half-topological state, and finally to the topologically trivial AFM state. Such phase transitions are absent in the models of correlated TIs with the Hubbard interaction [16–19].

Instead of the Chern number, the ground-state topology can also be detected by the crosses of the zeros of the diagonal topological Green function in the momentum space [40, 41]. The diagonal topological Green function is defined by

$$\hat{G}^{\gamma\gamma}_t(\mathbf{k},z)=\left[\frac{1}{z-\hat{H}_t(\mathbf{k})}\right]_{\gamma\gamma}=\sum_{\sigma\alpha}\frac{|\Phi^{(\gamma)}_{\sigma\alpha}(\mathbf{k})|^2}{z-E_{\sigma\alpha}(\mathbf{k})},\tag{13}$$

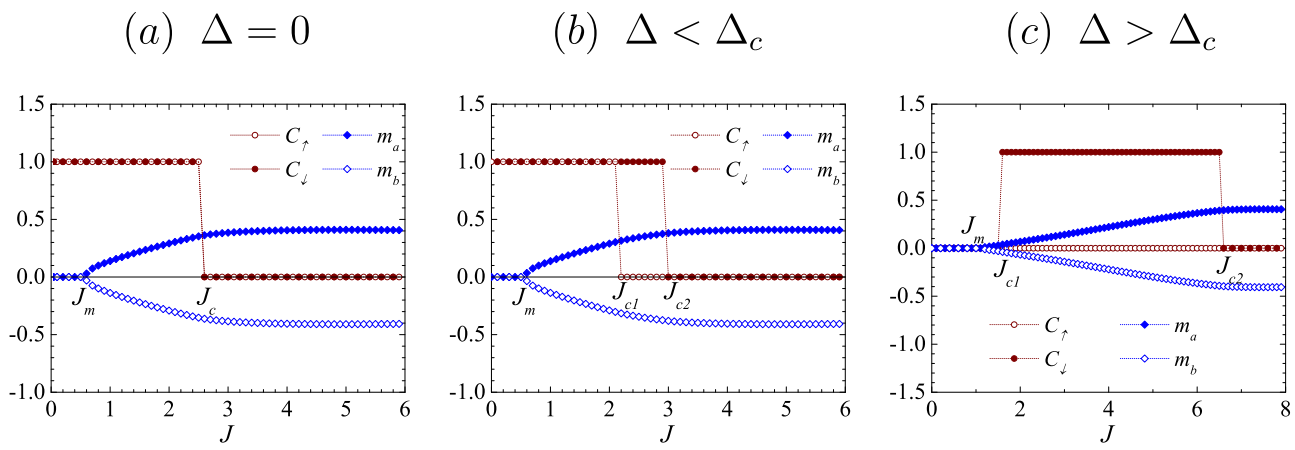

Figure 1. The Chern number C_σ for spin orientation σ and the sublattice magnetizations m_a, m_b via the Hund coupling J for different ionic potentials at fixed $t_2 = 0.5$ ($t = 1$). (a) $\Delta = 0$, (b) $\Delta = 1$, (c) $\Delta = 8$.

where $E_{\sigma\alpha}(\mathbf{k})$ and $|\Phi_{\sigma\alpha}(\mathbf{k})\rangle$ are the eigenvalue and eigenvector of the topological Bloch Hamiltonian $\hat{H}_t(\mathbf{k}) = \hat{H}_0(\mathbf{k}) + \hat{\Sigma}(i0)$, and $|\Phi^{(\gamma)}_{\sigma\alpha}(\mathbf{k})\rangle$ is the γth component of $|\Phi_{\sigma\alpha}(\mathbf{k})\rangle$ [40, 41]. The topological Bloch Hamiltonian $\hat{H}_t(\mathbf{k})$ determines the Chern number, as can be seen from the generalized TKNN formula (12) for interacting systems [45]. Based on the eigenvector-eigenvalue identity of Hermitian operator [47], it was shown that the zeros of the diagonal topological Green function cross in TIs, and they do not cross in normal insulators [40, 41]. Therefore, the zero's crosses are a signal of nontrivial topology of insulating ground state.

Within the DMFT the zeros of the diagonal topological Green function are simply determined. They read

$$\mathcal{E}^{(\gamma)}_\sigma(\mathbf{k}) = -\epsilon_{\bar{\gamma}} t_2 \xi_{\mathbf{k}} - \epsilon_{\bar{\gamma}} \Delta/2 + \Sigma_{\bar{\gamma}\sigma}(i0), \tag{14}$$

where the bar symbol denotes $\bar{a} = b$, $\bar{b} = a$. In figure 2 we plot the spectral function $\rho_{a\sigma}(\mathbf{k}, \omega) = -\mathrm{Im}\, G_{\alpha\sigma}(\mathbf{k}, \omega + i0^+)/\pi$ and the zeros $\mathcal{E}^{(\gamma)}_\sigma(\mathbf{k})$ of the diagonal topological Green function in three typical phase regions, when $\Delta < \Delta_c$ and $\Delta > \Delta_c$. The peaks of the spectral function describe the quasiparticle properties and their momentum dependence resembles the energy bands. Figure 2 clearly shows a gap which separates upper and lower bands for all values of J. The ground state is always insulating at half filling. The gap is opened by both the next-nearest-neighbor hopping t_2 and the Hund coupling J. When $J > J_m$, the spectral functions for spin up and spin down are different, and this is a signal of magnetic ordering. In the region $J < J_{c1}$, the zeros cross when $\Delta < \Delta_c$, and do not cross when $\Delta > \Delta_c$. The zero's crosses are consistent with the topology of the ground state. The ground state is topological when $\Delta < \Delta_c$, and is topologically trivial when $\Delta > \Delta_c$. In addition, in this region $J < J_{c1}$, the zeros of both spin orientations have the same crossing behavior. This implies that both spin orientations simultaneously form either topological (when $\Delta < \Delta_c$) or normal (when $\Delta > \Delta_c$) insulators. In the region $J_{c1} < J < J_{c2}$, only zeros of one spin orientation cross, while zeros of the opposite spin orientation do not cross. The zero's crosses in this region are also consistent with the topology of the ground state, and this yields the half topological state. In the region $J > J_{c2}$, the zeros of both spin orientations do not cross. This indicates that the ground state is topologically trivial. At the topological phase transition $J = J_{c1}$ or $J = J_{c2}$ the zeros of one spin orientation touch, as shown in figure 2. The touch points separate two regions of different crossing behaviours of the zeros. In one region the zeros cross, whereas in the other region they do not cross. The touch points also yield the gapless edge modes at the boundaries between two different topological phases. Figure 2 shows that the touch points of the zeros occur at the vertices $\mathbf{K}$ and $\mathbf{K}'$ of the Brillouin zone. Therefore, the half-topological state transition can be determined from the zero's touch points. In the AFM state, the self energy at zero frequency can be represented as

$$\Sigma_{\gamma\sigma}(i0) = \epsilon_\gamma \Sigma + \epsilon_\gamma \sigma \delta\Sigma, \tag{15}$$

where $\Sigma = [\Sigma_{a\uparrow}(i0) + \Sigma_{a\downarrow}(i0)]/2$, and $\delta\Sigma = [\Sigma_{a\uparrow}(i0) - \Sigma_{a\downarrow}(i0)]/2$ [40]. It is a combination of staggered nonmagnetic field Σ and staggered magnetic field $\delta\Sigma$. One can notice that when $\Delta = 0$, Σ vanishes. At the zero's touch points the zeros vanish. Therefore from equation (14) we obtain the equations which determine the phase transition points of the half-topological state. In the case $\Delta < \Delta_c$, we obtain

$$t_2 \xi_{\mathbf{K}} + \Delta/2 = \Sigma + \delta\Sigma, \tag{16}$$

$$t_2 \xi_{\mathbf{K}'} + \Delta/2 = \Sigma - \delta\Sigma, \tag{17}$$

and in the opposite case $\Delta > \Delta_c$, we obtain

$$t_2 \xi_{\mathbf{K}} + \Delta/2 = \Sigma - \delta\Sigma, \tag{18}$$

$$t_2 \xi_{\mathbf{K}'} + \Delta/2 = \Sigma - \delta\Sigma. \tag{19}$$

In equations (16)–(19), both quantities Σ and $\delta\Sigma$ depend on the Hund coupling J and the ionic potential Δ, as well as on the hopping parameters t, t_2. Equations (16)–(19) actually determine the half-topological state transition points J_{c1} and J_{c2} in the cases $\Delta < \Delta_c$ and $\Delta > \Delta_c$, respectively. When $\Delta = 0$, $J_{c1} = J_{c2}$, because $\xi_{\mathbf{K}} = -\xi_{\mathbf{K}'}$. Therefore, when $\Delta = 0$, electrons of both spin components simultaneously are in either topological or normal insulator. However, when the ionic potential and the Hund coupling are finite, Σ and $\delta\Sigma$ are

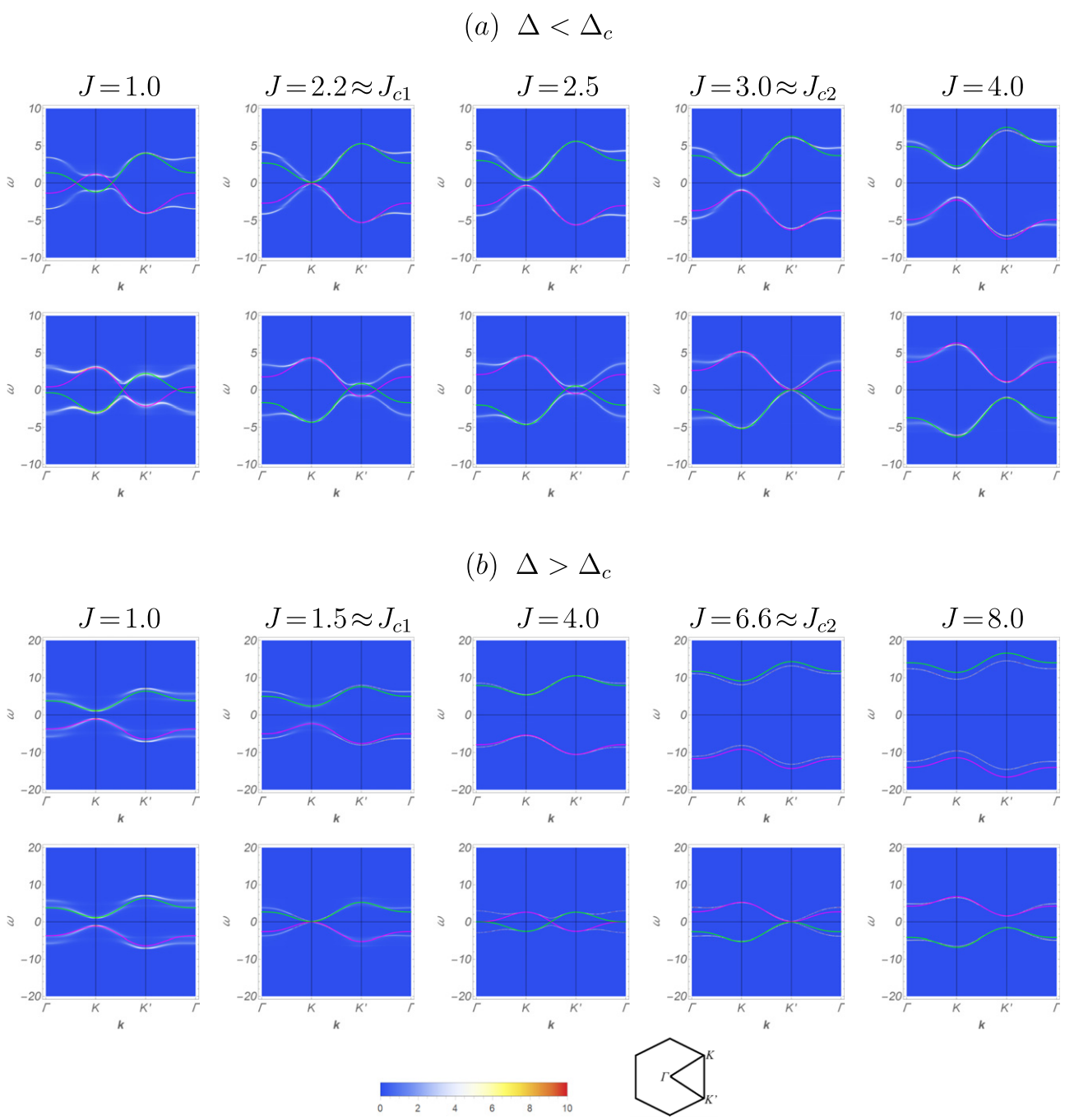

Figure 2. The color density plot of the spectral function of electrons and the color line plot of the zeros of the diagonal topological Green function (the green and magenta solid lines) along the high symmetry lines of the Brillouin zone for various values of the Hund coupling J, and $t_2 = 0.5$ ($t = 1$). The upper (lower) row presents the plots for the spin up (down) orientation. The color density plots only show the maximum values between the sublattice spectral functions. (a) $\Delta = 1$, (b) $\Delta = 8$.

also finite too. This leads to $J_{c1} \neq J_{c2}$. Therefore, the half-topological state occurs in the region $J_{c1} < J < J_{c2}$. It appears an emergence of the AFM magnetization and the breaking of the inversion symmetry. However, the AFM ordering and the breaking of the inversion symmetry are necessary, but not sufficient for the existence of the half-topological state. Instead of them, equations (16) and (17) or (18) and (19) determine the existence conditions of the half-topological state. The MTIs were experimentally observed, but there is no report of the half-topological state. It is a challenge for observing such half-topological state by experiments. The half-topological state may also be realized in artificial lattices simulated by using ultracold atoms or photonic technique. Indeed, the Haldane model was simulated by experiments using ultracold atoms [48]. Therefore, the spin version of the Haldane model may be simulated too. When an external field like the self energy in equation (15) is applied to the simulated lattice, the half-topological state would be observed. Equations (16) and (17) or (18) and (19) practically determine the value range of

the external field, where the half-topological state would be observed.

4. Conclusion

We have demonstrated a possibility of the half-topological state in AFM insulators. The half topological state is characterized by topologically breaking of the spin symmetry, when electrons with one spin orientation form a topological insulator and electrons with the opposite spin orientation form another insulator with trivial topology. The topologically breaking of spin symmetry occurs as an emergence of the AFM ordering and the lack of the inversion symmetry. However, the AFM ordering and the breaking of the inversion symmetry are necessary, but not sufficient for the existence of the half-topological state. We have also derived equations, which determine the phase transition of the half-topological state. They would practically determine the conditions for observing the half-topological state.

Acknowledgments

This research is funded by the International Centre of Physics (Institute of Physics, VAST) under Grant ICP.2021.03.

Data availability statement

The data that support the findings of this study are available upon reasonable request from the authors.

ORCID iDs

Minh-Tien Tran https://orcid.org/0000-0001-9579-3936

References

[1] Yu R, Zhang W, Zhang H-J, Zhang S-C, Dai X and Fang Z 2010 *Science* **329** 61
[2] Chang C Z *et al* 2013 *Science* **340** 167
[3] Li J *et al* 2019 *Sci. Adv.* **5** eaaw5685
[4] Zhang D, Shi M, Zhu T, Xing D, Zhang H and Wang J 2019 *Phys. Rev. Lett.* **122** 206401
[5] Weng H, Yu R, Hu X, Dai X and Fang Z 2015 *Adv. Phys.* **64** 227
[6] Hohenadler M and Assaad F F 2013 *J. Phys.: Condens. Matter* **25** 143201
[7] Rachel S 2018 *Rep. Prog. Phys.* **81** 116501
[8] Kohmoto M 1985 *Ann. Phys.* **160** 355
[9] Thouless D J, Kohmoto M, Nightingale M P and den Nijs M 1982 *Phys. Rev. Lett.* **49** 405
[10] Kane C L and Mele E J 2005 *Phys. Rev. Lett.* **95** 146802
[11] Tran M-T, Nguyen H-S and Le D-A 2016 *Phys. Rev.* B **93** 155160
[12] Tran T-M T, Le D-A, Pham T-M, Nguyen K-T T and Tran M-T 2020 *Phys. Rev.* B **102** 205124
[13] Haldane F D M 1988 *Phys. Rev. Lett.* **61** 2015
[14] de Groot R A, Mueller F M, van Engen P G and Buschow K H J 1983 *Phys. Rev. Lett.* **50** 2024
[15] Coey J M D and Venkatesan M 2002 *J. Appl. Phys.* **91** 8345
[16] Vanhala T I, Siro T, Liang L, Troyer M, Harju A and Törmä P 2016 *Phys. Rev. Lett.* **116** 225305
[17] Jiang K, Zhou S, Dai X and Wang Z 2018 *Phys. Rev. Lett.* **120** 157205
[18] Wang Y X and Qi D X 2019 *Phys. Rev.* B **99** 075204
[19] Ebrahimkhas M, Hafez-Torbati M and Hofstetter W 2021 *Phys. Rev.* B **103** 155108
[20] He J, Kou S-P, Liang Y and Feng S 2011 *Phys. Rev.* B **83** 205116
[21] He J, Zong Y H, Kou S P, Liang Y and Feng S 2011 *Phys. Rev.* B **84** 035127
[22] He J, Liang Y and Kou S-P 2012 *Phys. Rev.* B **85** 205107
[23] He J, Wang B and Kou S-P 2012 *Phys. Rev.* B **86** 235146
[24] Maciejko J and Rüegg A 2013 *Phys. Rev.* B **88** 241101
[25] Zener C 1951 *Phys. Rev.* **82** 403
[26] Anderson P W and Hasegawa H 1955 *Phys. Rev.* **100** 675
[27] Izyumov Y A and Skryabin Y N 2001 *Phys.-Usp.* **44** 109
[28] Metzner W and Vollhardt D 1989 *Phys. Rev. Lett.* **62** 324
[29] Georges A, Kotliar G, Krauth W and Rozenberg M J 1996 *Rev. Mod. Phys.* **68** 13
[30] Furukawa N 1994 *J. Phys. Soc. Japan* **63** 3214
[31] Furukawa N 1995 *J. Phys. Soc. Japan* **64** 2754
[32] Furukawa N 1996 *J. Phys. Soc. Japan* **65** 1174
[33] Yunoki S, Hu J, Malvezzi A L, Moreo A, Furukawa N and Dagotto E 1998 *Phys. Rev. Lett.* **80** 845
[34] Kogan E and Auslender M 2003 *Phys. Rev.* B **67** 132410
[35] Phan V-N and Tran M-T 2003 *Mod. Phys. Lett.* B **17** 39
[36] Minh-Tien T 2003 *Phys. Rev.* B **67** 144404
[37] Phan V-N and Tran M-T 2005 *Phys. Rev.* B **72** 214418
[38] Phan V-N and Tran M-T 2015 *Phys. Rev.* B **92** 155201
[39] Phan V-N, Ninh Q-H and Tran M-T 2016 *Phys. Rev.* B **93** 165115
[40] Tran M-T, Nguyen D-B, Nguyen H-S and Tran T-M T 2022 *Phys. Rev.* B **105** 155112
[41] Misawa T and Yamaji T 2021 arXiv:2102.04665
[42] Capponi S and Assaad F F 2001 *Phys. Rev.* B **63** 155114
[43] Volovik G E 1988 *Zh. Eksp. Teor. Fiz.* **94** 123 http://jetp.ras.ru/cgi-bin/e/index/r/94/9/p123?a=list
Volovik G E 1988 *Sov. Phys. JETP* **67** 1804 http://jetp.ras.ru/cgi-bin/e/index/e/67/9/p1804?a=list
[44] Gurarie V 2011 *Phys. Rev.* B **83** 085426
[45] Wang Z and Zhang S C 2012 *Phys. Rev.* X **2** 031008
[46] Fukui T, Hatsugai Y and Suzuki H 2005 *J. Phys. Soc. Japan* **74** 1674
[47] Denton P B, Parke S J, Tao T and Zhang X 2022 *Bull. Am. Math. Soc.* **59** 31–58
[48] Jotzu G, Messer M, Desbuquois R, Lebrat M, Uehlinger T, Greif D and Esslinger T 2014 *Nature* **515** 237